JOURNAL OF MATERIALS SCIENCE 35 (2000) 2145–2154

High-performance polymer coatings for carbon steel heat exchanger tubes in geothermal environments*

T. SUGAMA, R. WEBSTER, W. REAMS
Energy Efficiency and Conservation Division, Department of Applied Science, Brookhaven National Laboratory, Upton, New York 11973, USA
E-mail: sugama@bnl.gov

K. GAWLIK
National Renewable Energy Laboratory, 1617 Cole Boulevard, Golden, Colorado 80401, USA

The most critical issue in developing thermal conductive coatings for the interior surfaces of heat exchanger tubes made from mild carbon steel (MCS), which are used in geothermal power plants at temperatures ranging from 110° to 89°C, is the deposition of scales. These scales, induced by the brine, chemically adhere to the coating surfaces. One of the major factors governing the formation of a strong interfacial bond at interfaces between the coatings and scales was the brine-promoted hydrothermal oxidation of the coatings. In seeking coating unsusceptible to hydrothermal oxidation, two semi-crystalline thermoplastic polymers, polyphenylenesulfide (PPS) and polytetrafluoroethylene (PTFE)-blended PPS, were applied as interior surface coatings to the zinc phosphated MCS tubes. The PPS coating surfaces suffered some oxidation caused by their chemical affinity for $FeCl_2$ in geothermal brine. $FeCl_2$-promoted oxidation of PPS surfaces not only incorporated more oxygen into them, generating a sulfide → sulfone → sulfonic acid conformational transformation within the PPS, but also caused the disintegration of PPS, yielding fragmental polychloroaryl compound and ferrous sulfate ($FeSO_4$) derivatives. The $FeSO_4$ reaction product formed at the interfaces between the scale and PPS coating was soluble in water, so that the coatings could be easily removed by highly pressurized water. The oxidation of PPS was considerably inhibited by blending PTFE into it, forming coating surface unsusceptible to hydrothermal oxidation reactions with hot brine. The major reason for such inhibition of oxidation was the formation of a chemically inert PTFE layer segregated from the PPS layer at the outermost surface site of the coating. Hence, the scale easily flaked off from the PTFE-blended PPS coating surfaces. This characteristic of surface was similar to that of the stainless steel surfaces. Nevertheless, both PPS and PTFE-blended PPS coatings can be classified as scale-free coatings.

1. Introduction

Corrosion, erosion, and fouling by scale deposits are critical issues in using heat-exchanger tubes at geothermal binary-cycle power plants in the Salton Sea reservoir (California). Replacing these tubes is very costly and time consuming. At present, tubes and shell heat exchangers made from titanium alloys and stainless steels are commonly used for dealing with these problems in the power stations. However, these metals are considerably more expensive and have much lower thermal conductivities than copper and carbon steels. If an inexpensive tube of mild carbon steel (MCS) could be coated with a thermally conductive material that confers corrosion resistance equal to that of copper, brass, and high-grade alloy steels, then the capital cost of these large heat exchangers would be markedly reduced. Thus, the objective of our collaborative work with the National Renewable Energy Laboratory (NREC) is to develop and design anti-corrosion, -erosion, and -fouling coating systems with a high thermal conductivity for MCS-based heat exchanger tubes.

In our previous studies [1–3], we focused on investigating the usefulness of organic polymer-based composite material systems that provide an excellent thermal conductivity of 2.35×10^{-2} W/mK, about twice as high as that of single polymeric materials, as corrosion-protective and thermal-conductive interior surface coatings of the tubes. The composite coating system

*This program report issued by Raymond LaSala (Program Manager, DOE Geothermal Technology Division) was performed under the auspices of the U.S. Department of Energy.

consisted of the trimethylolpropane trimethacrylate (TMP)-crosslinked styrene/methyl methacrylate copolymers as the binder and the silicon carbide (SiC) filler as the thermal conductor. When this composite material was deposited on the interior surfaces of tubes by centrifuging placement technology, and then cured at 177°C, it displayed a heat transfer coefficient which was only 9% less than that of expensive stainless steel (AL-6XN), and also conferred resistance to corrosion of the steel. However, a major drawback of this liner was the fact that the functional ester (-COO-R) groups in the copolymer suffered hot brine-induced oxidation, forming a functional carboxylate (COO^-) derivative. This derivative preferentially reacted with Ba^{2+} ions, from among the chemicals present in the geothermal brines, to form Ba- complexed carboxylate hydrolysates. Such an introduction of complexed carboxylate compounds onto the copolymer surfaces promoted the rate of the deposition of brine-induced scales on the coating surfaces, thereby lowering their heat-transfer performance and increasing brine flow pressure losses. In addition, this reaction product formed at the interfaces between the coating and scale layers caused the scales to adhere strongly to the coating, making them difficult to remove from the coating surfaces. Contrarily, the scales that accumulated on the uncoated stainless steel were easily removed by highly pressurized water, thereby restoring their function as the heat exchanger tubes. Accordingly, a primary requirement for polymeric materials used in the coating systems is that they must be unsusceptible to oxidation reactions with a hot brine, so there is no chemical linkage of the polymeric coatings to the scales. Such chemical inertness of the coatings would offer improved surface properties ensuring that the scales could be removed from the coating surfaces.

To achieve this goal, three polymeric material systems, 1,4-phenylene diamine (PDA) antioxidant-containing TMP-crosslinked styrene/methyl methacrylate (TMP-ST) copolymers, polyphenylenesulfide (PPS), and polytetrafluoroethylene-blended PPS, were evaluated for use as corrosion- and oxidation-resistant coatings. The major characteristics of PPS and PTFE-blended PPS known as the high-temperature performance thermoplastics were the molecular orientation caused by chain extension at their melting point, and the absence of functional groups, such as ester, ketone, aldehyde, carboxylic acid, and alcohol, in the polymer structures. For the former characteristic, the molecular orientation, responsible for the semi-crystallization behavior of PPS and PTFE, gave them specific, desirable properties; they show high-temperature hydrothermal stability, chemical resistance, and excellent elongation properties [4]. Furthermore, PTFE employed as the blending material for PPS, not only conferred superior thermal and chemical stability, but also provided low surface energy and surface slip [5].

An ideal polymeric coating that protects steel from corrosion in geothermal environments must act as a barrier against corrosive reactants, such as oxygen, water, electrolyte species (e.g., H^+, Na^+, Cl^-, SO_4^{2-}, NO_2^-), and gases (e.g., O_2, SO_2, CO_2, H_2S). Unfortunately, all polymeric coatings are permeable to these reactants in some different degree [6]. A major consideration is that when the reactant reaches the steel surfaces beneath the coating layers, corrosion occurs at interfaces between the polymer and steel. Once corrosion starts, the growth of corrosion products at the interfaces promotes wedging and blistering, which puts tremendous stress on the interfacial side of the coating film; consequently, there is localized delamination and buckling of the stressed coating layers. Thus, it is very important to tailor the interface to inhibit the onset of the cathodic reaction. For tailoring material systems, zinc or zinc alloy and zinc phosphate (Zn.Ph) conversion precoatings are often introduced into the intermediate layers to pretreat the steel surfaces [7]. We demonstrated that the bond structure of PPS/zinc phosphated steel joint systems has both mechanical interlocking and chemical bonds [8]. The latter was characterized by representation of the formation of zinc sulfide (ZnS) reaction products yielded by chemical interactions between PPS and the Zn in the Zn.Ph layer during exposure to a wet, harsh environment. Such combined mechanical and chemical bonds significantly enhanced the force of the Zn.Ph-to-PPS adhesion, thereby resulting in a failure mode in which the loss of adhesion occurs through the mixed layers of Zn.Ph and the reaction products.

Based upon this information, three coating systems, SiC/PDA-TMP-ST/Zn.Ph, SiC/PPS/Zn.Ph, and PTFE-PPS/Zn.Ph, were applied to the interior surfaces of the MCS tubes, 25 mm outside diam. × 1.2 mm wall thickness × 6100 mm long, then, the tubes were exposured to flowing hypersaline brine for 45 days in a geothermal power plant at temperatures up to 110°C. The bare stainless steel (AL-6XN) tube ends (50 mm long), which were jointed to the tubesheets by a roller expansion process, were used as the uncoated controls. Regarding the heat-transferable property of these coating systems, the thermal conductivity of PTFE-blended PPS coating without SiC grits was somewhat lower than that of the SiC-filled PPS coating [9]. Although all the coatings greatly protected the underlying MCS tubes against corrosion induced by the hot hypersaline brine, the scales were deposited on all of them, including the stainless steel tube ends. Thus, our present work was directed towards a fundamental understanding of the chemistry at the interfaces between the coatings and the scales after such exposure. We focused on the following three objectives: (1) investigating the degree of oxidation of the coating surfaces, and exploring the microstructure that developed in the critical interfacial regions between the coating and scale; (2) identifying the reaction products formed by interaction at these interfaces, and modeling their interaction pathways; and (3) determining the shear-bond strength of the scale-to- coating joint specimens. The integration of all the data would provide the information on the most effective coating systems in minimizing the degree of oxidation, forming the scale-free coating surfaces.

2. Experimental

2.1. Materials

The mild carbon steel (MCS) tubes, 6100 mm lengths of 25 mm outside diam. by 1.2 mm wall thickness,

were used in this study. A 50 mm stainless steel (SS, AL-6XN) stub was welded to each end of the tube to provide the safe end connection to the tubesheet. The 25 mm of each stub was left uncoated to provide a location for roller expanding the safe end to the tubesheet. Three vinyl-type monomers, styrene (ST), trimethylolpropane trimethacrylate (TMP), and methyl methacrylate (MMA), were used as starting materials for the TMP-crosslinked ST/MMA copolymer binder. Three catalysts, dimethyl aniline (DMA), di-tert-butylperoxide (DTBP), and benzoyl peroxide (BPO), were added to this monomer blend to initiate its polymerization. The "as-received" PPS powder for the slurry coating, supplied by the Phillips 66 Company, was a finely divided, tan-colored powder having a high melt flow at its melting point of 290°C. The PTFE powder (commercial grade, SST-3H), supplied by Shamrock Technologies Inc., was used as a slip-enhancing and oxidation-resistant additive to PPS. PTFE-blended PPS powders, with PPS/PTFE ratios of 89/11 by weight, were prepared in a rotary blender. The blended and unblended PPS powders were mixed with the isopropyl alcohol to make the slurry coatings. Before depositing these coatings on the interior surfaces of the MCS tubes, the tubes were covered with a zinc phosphate (Zn.Ph) coating. The Zn.Ph coating is applied using a "fill and drain" technique. The tube is coated by attaching a valve to one end of the tube and then inserting it into a vertically oriented furnace. The coating solution consisting of 5.0 wt% zinc orthophosphate dihydrate, 10.0 wt% H_3PO_4, 1.0 wt% $Mn(NO_3)_2$. $6H_2O$, and 84.0 wt% water is poured into the tube from the top, and then drained from the bottom once the coating process is completed. The steps in this process are as follows: (1) insert the tube into the vertical furnace, (2) pre-heat the tube to 80°C, (3) pre-heat the Zn.Ph solution to 80°C, (4) fill the tube with the Zn.Ph solution and maintain the filled tube at $80°C \pm 5°$ for 30 min., (5) drain the solution from the tube and wash the interior with 80°C water, and (6) bake the Zn.Ph-treated tube at 125°C for 1 hr to form the anhydrous Zn.Ph coating. The silicon carbide (SiC) grits used to enhance the thermal conductivity of the polymers were of three different sizes, ∼142, ∼32, and ∼9 μm. These SiC grits were blended in the following proportion: ∼142 μm : ∼32 μm : ∼9 μm = 50 wt% : 25 wt% : 25 wt%, before incorporating them into the polymers.

2.2. Coating technologies

The PDA-modified TMP-ST/SiC system is a polymer composite system consisting of 18 wt% monomer and 82 wt% SiC grit. The formulation of the PDA-containing TMP-ST monomer system is 53 wt% styrene-polystyrene mixture, 35.3 wt% TMP, 4.8 wt% poly(methyl methacrylate), 1 wt% silane coupling agent, 1 wt% DTBA promoter, and 2.4 wt% BPO ambient and 2.4% DMA high temperature initiators, and 0.1 wt% PDA antioxidant.

The PDA-modified TMP-ST/SiC coating is centrifugally cast inside the zinc phosphate-treated tubing using the following procedure: (1) The tube is inserted into the spinning assembly and locked into position. The monomer/SiC mixture is then poured into the tube and distributed along its length using a screed designed to uniformly distribute enough material along the length of the tube. (2) The tube is slowly rotated to allow the mix to fully coat the interior surface. The drive motor speed is then gradually increased to 600 rpm and the tube is spun for 4 hr to compact the liner against the tubing and to allow the liner mixture to take its initial set. (3) Once the spinning has been completed the tube is post-cured in a two-step curing process. The first step involves spinning the tube at 80°C for 2.5 hr to complete the initial curing of the liner. This is accomplished by placing an enclosure over the spinning assembly and heating the enclosed air. The tube is then removed from the spinning assembly and placed inside a curing chamber where it is second cured at a temperature of 175°C for 4 hr.

The SiC-filled PPS coating is applied using the "fill and drain" technique. The PPS system consists of two layers of PPS while the PPS/SiC system consists of one layer of PPS and a top layer of SiC-filled PPS. The steps in the coating process are as follows: (1) insert the zinc phosphated tube into the vertical furnace, (2) coat its interior by filling it with a slurry of 50 wt% PPS, 49 wt% isopropyl alcohol, and 1 wt% surfactant, (3) drain the slurry from the tube, (4) leave the slurry-coated tube to stand for 1 hr to allow the alcohol to evaporate, (5) pre-heat the tube to 125°C drive off any remaining alcohol then raise the temperature of the tube to 320°C and maintain it at this level for 3 hr to cure and crosslink the PPS, (6) allow the tube to cool to room temperature, and then repeat the entire process to apply a second coat of the SiC-filled PPS. The formulation of the slurry for the SiC-filled PPS is 36 wt% PPS, 45 wt% isopropyl alcohol, 1 wt% surfactant, and 18 wt% SiC grit.

The PTFE-blended PPS coating without SiC is also applied using the "fill and drain" technique. This coating system is composed of two layers similar to that of the SiC-filled PPS coatings; one layer is a single PPS as underlying coating, and the top coating is the PTFE-blended PPS. The coating process was accomplished in the steps similar to those used in making the SiC- filled PPS coatings, except for the step (6). In the step (6), the formulation of the slurry used as the top coating was 41 wt% PPS, 5 wt% PTFE, and 54 wt% isopropyl alcohol. This slurry was applied to the underlying PPS coating surfaces, and then heated at 320°C to achieve its melt flow, and subsequently cooled to room temperature to make a solid film. The thickness of these coating systems was ∼0.85 mm for SiC-filled PDA-TMP-ST-Zn.Ph, ∼0.3 mm for SiC-filled PPS-Zn.Ph, and ∼0.28 mm for PTFE-blended PPS-Zn.Ph. Although an intuitively, thicker coating may be expected to have a better corrosion-protective performance than a thin one, these coating systems were used to quantify their effectiveness.

2.3. Measurements

The coated MCS tubes with uncoated SS tube ends were exposed to flowing hypersaline brine for 45 days in a geothermal power plant. Table I shows the chemical

TABLE I Chemical compounds and composition of brine

Major elements	Compounds	Percent
Chloride	Various metal chlorides	13.5
Sodium	NaCl	6.0
Calcium	CaCl	3.0
Potassium	KCl	1.5
Minor elements	*Compounds*	*PPM*
Carbon dioxide	CO_2	2000
Iron (ferrous)	$FeCl_2$	1000
Manganese	$MnCl_2$	930
Strontium	$SrCl_2$	430
Ammonia	NH_3	420
Lithium	LiCl	410
Zinc	$ZnCl_2$	370
Boron	H_3BO_3	330
Silicon	SiO_2	250
Barium	$BaCl_2$	130
Hydrogen sulfide	H_2S	70

compounds and composition of the Salton Sea brine, collected by CalEnergy Operating Company on June 1, 1995. The exposure test was carried out by NREL. The heat exchanger had an inlet temperature of about 109°C and an inlet pressure of about 6.5×10^5 Pa, while the average outlet temperature and pressures were 89°C and 4.8×10^5 Pa, respectively. Visual observation of all the tubes after exposure revealed that scale had deposited on the internal coating and SS surfaces. The microstructure developed in the critical interfacial regions between the scale and coating or SS layers and their chemical compositions were explored using scanning electron microscopy (SEM) and energy-dispersive x-ray spectrometry (EDX). The shear-bond strength for 75 mm-long samples cut from selected areas of the exposed tube specimens was determined to assess the adherence of scales to the coating and SS surfaces. The chemical compositions on both the interfacial scale and coating or SS failure sides were investigated by examining the binding energy (BE) deduced from x-ray photoelectron spectroscopy (XPS). The atomic fractions for the respective chemical elements were estimated by comparing the XPS peak areas, which can be obtained from differential cross-sections for core-level excitation. To set a scale in the high-resolution XPS spectra, the binding energy was calibrated with the C_{1s} of the principal hydrocarbon-type carbon peak fixed at 285.0 eV as an internal reference [10]. A curve deconvolution technique, using a DuPont curve resolver, revealed the chemical components from the high-resolution spectra of each element. In addition, since the PPS and PTFE materials used have the thermoplastic characteristics, the thermal properties including the endothermic melting point and the exothermic crystallization temperature of PTFE-blended and unblended PPS polymers were investigated by differential scanning calorimetry (DSC) in air. DSC was run using the non-isothermal method at a constant rate of 10°C/min over the temperature range of 25° to 450°C.

3. Results and discussion

Table II shows the thickness of geothermal brine-induced scales deposited over the coating surfaces and the shear bond strength at the interfaces between the coatings and the scales: there was no significant difference in the thickness of scale between them. Their thickness ranged from ∼1.8 to ∼2.3 mm. The shear bond strength, an average value from six specimens, was used to estimate the adhesive force of the scales to the coating and SS surfaces. The adherence of scales to the SiC-filled PDA-TMP-ST-Zn.Ph (PTSZ) coating surfaces was considerably higher than that to uncoated stainless steel (SS) surfaces. The bond strength of 8.20 MPa for the scale/SiC-filled PTSZ joint specimens was almost seven times greater than that of the scale/SS joints. The weak interfacial boundary for the scale/SS joint makes it easy to dislodge and remove the scales from the SS surfaces using highly pressurized water in terms of the hydroblast, whereas it was very difficult to dislodge the scales in the scale/SiC-filled PTSZ joint system. Thus, conceivably, the effectiveness of the PDA antioxidant in creating chemically inert coating surfaces to the scales was very little, if any. In fact, the SEM-EDX and FT-IR analyses (data are not shown) of cross-sectional areas of the scale/coating joints revealed findings similar to those of the scale/SiC-filled TMP-ST coating joint systems without PDA, described in a previous paper [3]; namely, the formation of Ba-complexed carboxylate salts yielded by hydrothermal reactions between ester groups in the polymer and Ba ions in brine was identified in the critical interfacial boundary regions between coatings and scales. Hence, we made no further investigations of the characteristics of this joint specimen.

TABLE II The thickness of scale deposited on coating surfaces and the shear bond strength at interfaces between coatings and scales

Joint system	Thickness of scale, mm	Shear bond strength, MPa
Scale/SS	∼2.1	1.21
Scale/SiC-filled PTSZ	∼2.1	8.20
Scale/SiC-filled PPS	∼2.3	5.82
Scale/PTFE-blended PPS	∼1.8	1.59

Using the SiC-filled PPS-Zn.Ph coatings, their joint systems had a shear bond strength of 5.82 MPa, corresponding to an ∼71% decrease compared to that of the scale/SiC-filled PTSZ coating joint specimens. This low bond strength was responsible for the formation of scale layers over the coating surfaces removable by hydroblast. A considerably lower bond strength of 1.59 MPa was determined from the scale/PTFE-blended PPS-Zn.Ph coating joints. This value was almost equal to that of the scale/SS joint specimens, strongly suggesting that the surfaces of the PTFE-blended PPS have very similar characteristics to those of the SS surfaces which were unsusceptible to hydrothermal oxidation reaction by geothermal brine.

From these results, our focus centered on gaining a fundamental understanding of chemistry at the interfaces between the PTFE-blended PPS or unblended PPS polymer coatings and the scales. Before starting exploration of the interfacial chemistry, we investigated the thermal behavior of these thermoplastic polymers.

Considering the repeated melting-crystallization behaviors of a single PPS and PTFE-blended PPS polymers, the cyclic DSC curves of these polymers were investigated at a heating-cooling rate of $\pm 10^{\circ}$C min^{-1} and at temperatures ranging from 25° to 450°C in air. Samples were prepared as follows: Open aluminum DSC pans were filled with ~5 mg slurries containing three components, the PPS, PTFE, and isopropyl alcohol, and then placed in an oven at 450°C in air for 3 hours. The melted samples were subsequently cooled to room temperature at the rate of $\sim -10^{\circ}$C min^{-1}; the pans were then sealed with aluminum covers. The sealed samples were heated again to 450°C at the rate of $+10^{\circ}$C min^{-1} and immediately cooled to 90°C at the rate of -10°C min^{-1}. Cooling from 450°C to low temperature was accomplished using a DuPont mechanical cooling accessory equipped with a DSC.

The resulting cyclic DSC curves for the PPS/PTFE ratios of 100/0 and 89/11 are illustrated in Fig. 1. The typical thermodynamic DSC scan (a) for the unblended PPS, denoted as a 100/0 ratio, had endothermic peak at ~260°C, reflecting its melting point, T_{m1}. On cooling the melted polymer, an exothermic peak, T_{c1}, was recorded around 170°C, which represents the heat evolved during the crystallization of PPS. By comparison, the curve (b) of the blended PPS with 89/11 ratio disclosed two endothermic peaks at ~260°C and ~320°C. Since the first peak is associated with the melting point of PPS, it is possible to assume that the second one, T_{m2}, represents the melting point of PTFE. Correspondingly, the appearance of two exothermic peaks at ~170° and ~310°C is reasonably thought to be due to the crystallization point, T_{c1} and T_{c2}, of PPS and PTFE, respectively. Thus, there is no clear evidence for the formation of reaction products yielded by interactions between the PPS and PTFE in the melting-flowing processes. In other words, if PPS chemically reacts with PTFE, a new peak related to the reaction products should have appeared at a different temperature from these ones.

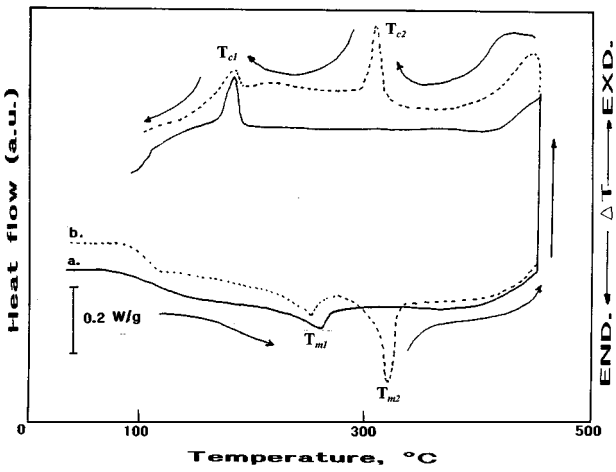

Figure 1 Cyclic DSC curves for polymers with PPS/PTFE ratio of 100/0 (a) and 89/11 (b).

The chemical compositions on both of the separated-interfacial scale and coating or SS sides after shear bond testing were investigated by XPS to gain an understanding of interfacial chemistry. All the XPS measurements were made at an electron-take-off angle of 40°, which corresponds to an electron-penetration depth of ~5 nm. Table III gives the surface atomic fraction obtained from XPS survey scan of the separated surfaces (both scale and coating or SS sides). The resulting fraction data are the average of numbers taken from four different locations of the sample surfaces. Atomic fractions for the bulk scale, PPS, PTFE-blended PPS, and SS surfaces are also included for comparison. The scale reference samples had seven major atoms, Si, S, C, Cl, Ca, O, and Fe, and four minor ones, Cr, Mn, Cu, and Ba. The oxygen, sulfur, chlorine, and carbon elements may be associated with oxide, sulfate, sulfide, chloride, and carbonate compounds in the scales. As expected, only three atoms, S, C, and O, were detected from the PPS reference surfaces; the O may be incorporated into the PPS during its melting-flowing process at 350°C in air. In contrast, the chemical composition of blended PPS polymer surfaces showed two principal atoms, F and C, while S and O atoms are present as minor elements. This data suggests that almost the entire surface of blended PPS polymers is covered by PTFE polymer because of the presence of F and C as the dominant atoms. The SS surfaces consisted of C and O as primary components, and Cr, Mo, Fe, and Ni as secondary ones. Comparing this with the reference SS samples, a striking difference in atomic fraction was observed from the interfacial SS side in the scale/SS joint systems; several new atoms are present, such as Si, S, Cl, Ca, Mn, Cu, and Ba. It

TABLE III Atomic fraction of both interfacial failure sides after shear bond tests for scale/SS, /SiC-filled PPS and /PTFE-blended PPS joint systems

		Atomic fraction, %													
Joint system	Failure side	Si	S	F	C	Cl	Ca	O	Cr	Mn	Mo	Fe	Cu	Ba	Ni
Scale surface	—	15.3	8.6	0.0	12.2	6.4	12.6	28.4	1.0	2.1	0.0	8.7	1.2	3.5	0.0
PPS surface	—	0.0	13.0	0.0	81.6	0.0	0.0	5.4	0.0	0.0	0.0	0.0	0.0	0.0	0.0
PTFE-PPS surface	—	0.0	2.5	48.8	45.7	0.0	0.0	3.0	0.0	0.0	0.0	0.0	0.0	0.0	0.0
SS surface	—	0.0	0.0	0.0	68.1	0.0	0.0	25.9	1.9	0.0	0.7	2.6	0.0	0.0	0.8
Scale/SS	SS	2.3	1.2	0.0	65.3	0.8	2.8	19.7	1.3	0.8	0.4	3.1	0.4	1.4	0.5
Scale/SS	Scale	16.9	7.3	0.0	12.8	6.1	12.2	32.0	1.7	1.3	0.0	6.0	1.1	2.6	0.0
Scale/SiC-PPS	Coating	4.4	3.0	0.0	51.1	5.0	2.1	21.7	1.7	0.9	0.0	7.2	0.9	2.0	0.0
Scale/SiC-PPS	Scale	13.7	6.8	0.0	14.4	5.8	11.1	34.2	1.6	1.8	0.0	6.4	1.1	3.1	0.0
Scale/PTFE-PPS	Coating	0.0	2.7	47.3	42.0	0.0	0.0	6.2	0.0	0.0	0.0	1.8	0.0	0.0	0.0
Scale/PTFE-PPS	Scale	14.7	7.9	0.0	13.5	6.0	12.0	31.8	0.7	1.9	0.0	7.3	1.0	3.2	0.0

appears that these atoms were transferred to the SS side from the scale during the failure of interfacial bonds. However, the amount of these scale-related atoms left on the SS side were very small. No SS-related atoms were detected on the interfacial scale side opposite to the SS. Thus, the loss of adhesion in this joint system was generated by two failure modes: One mode was the cohesive failure in which disbondment occurs through the scale layers; the other one called adhesive failure was related to the bond failure at the interface between the SS and the scale. In fact, the SEM image (not shown) of this surface revealed a random distribution of scale particles adhering to the SS surfaces. In the scale/SiC-filled PPS joint systems, the chemical composition on the coating interfaces separated from the scale had a 4.4% Si, 3.0% S, 51.1% C, 5.0% Cl, 2.1% Ca, 21.7% O, 1.7% Cr, 0.9% Mn, 7.2% Fe, 0.9% Cu, and 2.0% Ba. Although some Si, S, C, and O atoms arise from the SiO_2-filled PPS coatings, almost all the atoms belong to those of the scales. Interestingly, this composition, except for the coating-related atoms, and Fe and Cl, closely resembled that of the SS interfaces in the scale/SS joint system, implying that bond failure at the scale/coating joints includes the two modes described above, a cohesive one and adhesive one. The combination of such failure modes is the reason why the shear bond strength of these joint specimens is ∼71% lower than that of the scale/SiC-filled PTSZ coating joints.

Next, the focus centered on answering one important question: Why more Fe and Cl is left on the coating surfaces, compared with that of the other scale-related atoms, such as Si, S, Ca, Cr, Mn, Cu, and Ba. In response to this question, the approach to identifying the Fe- , S-, and Cl-related chemical states in the critical interfacial boundary regions between scale and coating layers was made by inspecting the high-resolution XPS spectra of S_{2p}, Fe_{2p}, and Cl_{2p} core-level excitations for the interfacial coating side. Such identification might resolve the question of why the Fe and Cl atoms preferentially transfer to the coating side from the scale during the failure of interfacial bonds. If these atoms chemically react with the coating, these reaction products would be identified from XPS data; giving us information on the reaction pathways that generate these reaction products. The XPS S_{2p} region (Fig. 2) on the interfacial coating side indicated the presence of four resolvable peaks: One is principal peak at 163.4 eV as the major component; the other three peaks were related to the excitation at 167.2, 169.2, and 169.9 eV as the minor ones. The major peak is attributable to the S in

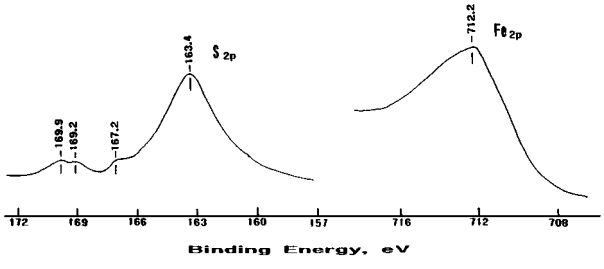

Figure 2 XPS S_{2p} and Fe_{2p} regions of SiC-filled PPS coating site removed from scales.

PPS [11]. An XPS study on sulphur-oxygen bonds [12, 13] suggested that an increase in the rate of oxidation of S results in a shift in peak position to a high BE site; for instance, sulfoxide (>S=O) at 165.9 eV, sulfone ($>SO_2$) at ∼167.5 eV, sulfonic acid ($-SO_3H$) at ∼169.0 eV, and sulfate ($-SO_4$) at ∼170.0 eV. From this information, we assume that the contributors to the excitations at 167.2, 169.2, and 169.9 eV are associated with the sulfone, sulfonic acid, and sulfate groups, respectively. If these assignments are valid, the sulfone group could be formed by the oxidation of sulfide group within the PPS. A further oxidation of polysulfone might lead to conformational transformation into the polysulphonic acid, seemingly verifying that the PPS surfaces are susceptible to hydrothermal oxidation reaction with geothermal brine. One question remains that must be answered affirmatively: What is the sulfate-related compound contributing to the peak at 169.9 eV? Since the Fe is the most predominant metallic element detected on the interfacial coating side, this finding suggests that two iron-related sulfate compounds, ferric- and ferrous-sulfates, might be formed. In trying to identify the contributor to this peak, two reference Fe compounds, iron (II) sulfate heptahydrate ($FeSO_4 \cdot 7H_2O$) and iron (III) sulfate pentahydrate [$(Fe_2(SO_4)_3 \cdot 5H_2O$], were inspected; the peak position in their S_{2p} spectra was 169.8 and 170.2 eV, respectively. Accordingly, the core line at 169.9 eV is more likely to be associated with S in the ferrous sulfate ($FeSO_4$), rather than in the ferric sulfate. Also, inspecting the XPS Fe_{2p} region of this sample supported the formation of the $FeSO_4$ as the reaction product. In fact, the Fe_{2p} core-level spectrum (Fig. 2) had the main peak at 712.2 eV, originating from Fe in the $FeSO_4$ [14]. As discussed earlier, the Fe-related compound in geothermal brine is ferrous chloride (Table I). Thus, we postulated that $FeSO_4$ was formed by the interaction between PPS and $FeCl_2$ in the brine. Since this reaction product is soluble in water, it can be dislodged from the coating surfaces by water. Although there is no experimental evidence on whether these derivatives are formed directly or indirectly, the following hypothetical hydrothermal oxidation pathway of the PPS may account for these observed conformational changes:

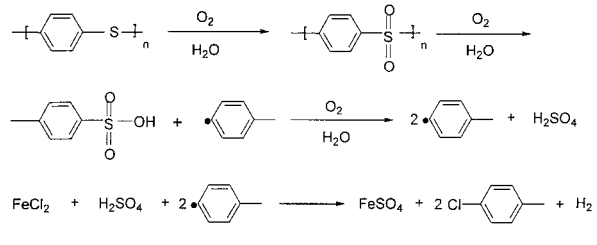

First, the sulfide → sulfone conformational change may take place in the hydrothermally oxidized PPS structure. A second hydrothermal oxidation process leads to the transformation of polysulfone into the polysulfonic acid, causing the breakage of the S−C bond in aryl sulfone which yields a fragmental aryl radical derivative. A further enhanced oxidation promotes the hydrothermal decomposition of polysulfonic acid, forming the other

fragmental derivatives, the aryl radical and H_2SO_4. Finally, H_2SO_4 favorably reacts with $FeCl_2$ to form $FeSO_4$; meanwhile, the Cl^- ion as a counter ion of Fe^{2+} may react with the aryl group having a free radical. This reaction may result in the formation of polychloroaryl compounds [15, 16]. Again, the XPS Cl_{2p} core-level spectrum of this specimen was investigated to ascertain whether or not the chloroaryl group is actually yielded in an oxidized PPS conformation. The spectrum (not shown) verified that this group forms in the oxidized PPS because of the excitation of a marked peak at 201.3 eV, originating from Cl in the chlorobenzene compounds [17]. From this oxidation pathway, $FeCl_2$ might act to promote the rate of its hydrothermal oxidation. We note that although H_2SO_4 may have a chemical affinity for the other scale-related chlorides, such as $CaCl_2$, $CrCl_2$, $MnCl_2$, $CuCl_2$, and $BaCl_2$, it was very difficult to identify these metal-associated sulfate compounds in these core-level excitations because of the very small amount of these metals that migrated from the brine to the coating.

To visualize insight into the morphological features of both the interfacial coating and scale sides, we surveyed the development of microstructure and elemental distribution for these interfacial samples by SEM-EDX. Fig. 3 shows the SEM image and EDX spectra taken from the interfacial coating sites in the scale/SiC-filled PPS joint system. As is seen, the image revealed two discernible microtextures: One was a smooth surface morphology denoted as site "a"; the other, site "b", expressed randomly distributed solid particles covering the coating surfaces. The EDX spectrum from site "a" included a pronounced signal of S, moderately intense signals of Cl and Fe, and less intense signals of O, Si, Ca, and Ba elements. The major element S appears to originate from the PPS. The Fe and Cl as the secondary elements may be assignable to the reaction products formed by hydrothermal oxidation reaction between the PPS and $FeCl_2$. In contrast, three prominent signals, O, S, and Fe elements were detected from the agglomerated particle areas of site "b". Although some S elements belong to the underlying PPS coating, there is no doubt that the contributor to these elements was the $FeSO_4$ reaction product. This spectrum also exhibited the presence of Si, Cl, Ca, and Ba. Thus, this information substantially supported the two experimental evidences described earlier: One was that the preferential uptake of $FeCl_2$ by PPS promotes the degree of its hydrothermal oxidation; the other one was that interfacial bond failure takes place through the two disbondment modes, adhesive failure occurring at interfaces between PPS and scale, and cohesive failure generated in the interfacial reaction products. Fig. 4 is the SEM image of the interfacial scale side opposite to the coating. Its morphological feature was characterized by representing a dense microstructure. As expected, the EDX spectrum had seven signals, O, Si, S, Cl, Ca, Ba, and Fe, as the representative elements of the scales.

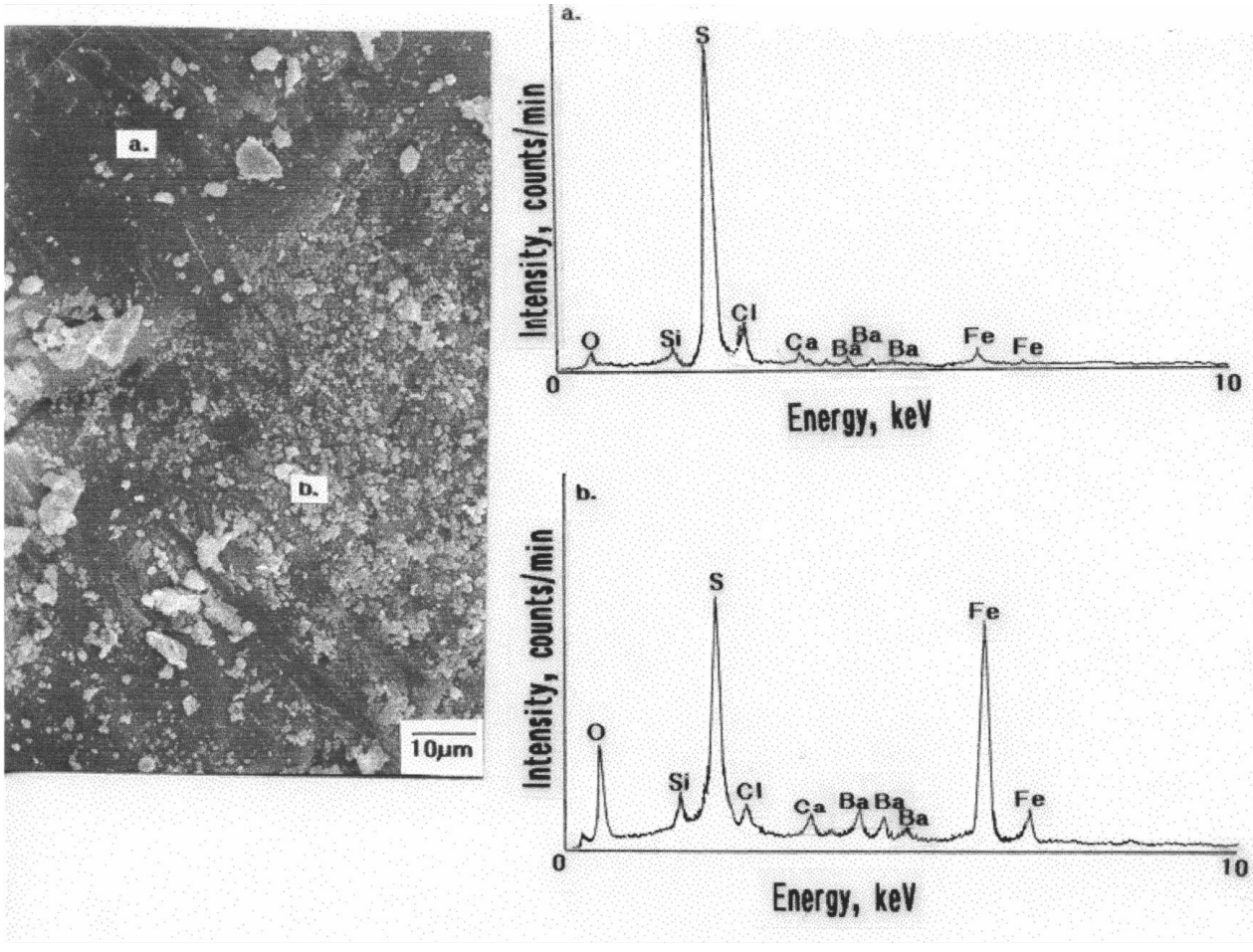

Figure 3 SEM image and EDX spectra for interfacial coating side in the scale/SiC-filled PPS coating joint specimens.

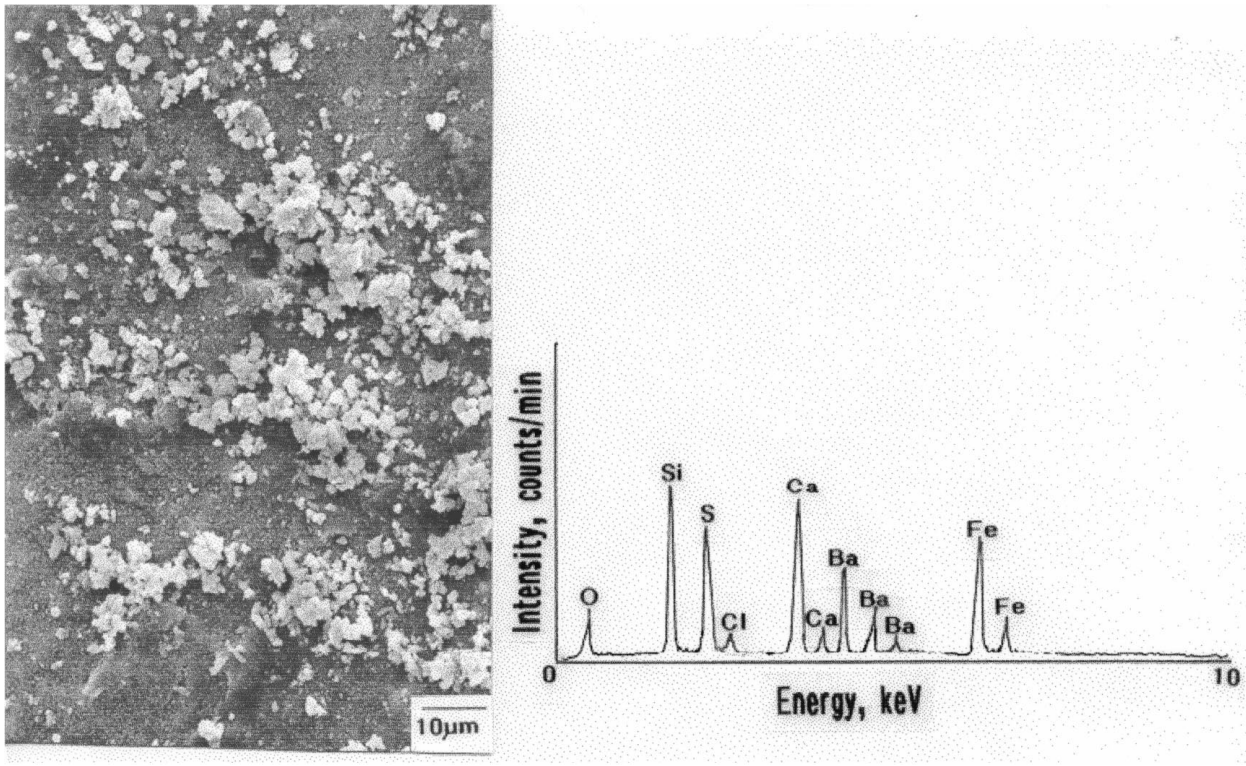

Figure 4 SEM-EDX analysis for interfacial scale site at the scale/SiC-filled PPS coating joint.

Returning to Table III, in the scale/PTFE-blending PPS joint system, there was a striking difference in the atomic composition of the interfacial coating side, from that in the scale/ SiC-filled PPS joint system; in particular, 1) there were no scale-related atoms, except for a very exiguous amount of Fe, 2) 89.3% of the total chemical composition was occupied by two elements, F and C, and 3) the degree of its oxidation was very low because of the incorporation of only 6.2% oxygen into the coating surface layer. For the differences (2) and (3), since the F and C atoms are attributable to the PTFE layer segregated from the PPS layer, these findings clearly demonstrated that the surface of the PTFE-blended PPS coating offers improved resistance to hydrothermal oxidation. In other words, PTFE occupping at the outermost surface site of the coating layer not only played important role in inhibiting the hydrothermal oxidation of the PPS coatings, but also in creating the chemically inert surfaces to the scale, enabling the coating surfaces to dislodge scales more easily than that of the unblended PPS coating. This is the reason why the shear bond strength at the scale/PTFE-blended PPS joints is much lower than that at the scale/SiC-filled PPS joints.

To support these information, the PTFE-blended and unblended PPS coating films were exposed for 21 days to 1 M solution of each of four representative geothermal chemical compounds, NaCl, $CaCl_2$, $FeCl_2$, and $BaCl_2$ at 200°C. Although the chemcial compounds of the geothermal brine (Table I) showed that the concentrations of several chlorides, KCl, $MnCl_2$, $SrCl_2$, LiCl, and $ZnCl_2$, are higher than that of $BaCl_2$, our XPS and EDX analyses of the scale interfaces revealed the presence of a substantial amount of Ba. Hence, we selected the $BaCl_2$ from among the other representative chlorides. Also, the hydrothermal temperature of 200°C was employed to accelerate the degree of hydrothermal oxidation of the film surfaces brought about by the attack of these chlorides. The exposed film surfaces were then inspected by XPS to obtain information on the changes in the atomic composition, especially for the amount of oxygen relating to the degree of film's oxidation. The results from these samples were shown in Tables IV and V. When unblended PPS films

TABLE IV Chemical composition of PPS surfaces after exposure for 21 days to 1 M various chloride reactants at 200°C

Chloride reactant	Atomic fraction, %								Atomic ratio, O/C
	S	C	O	Na	Fe	Ba	Cl	Ca	
Control[a]	13.0	81.6	5.4	0.0	0.0	0.0	0.0	0.0	0.07
D.I. water	10.4	78.4	11.2	0.0	0.0	0.0	0.0	0.0	0.14
NaCl	9.1	77.1	13.1	0.4	0.0	0.0	0.3	0.0	0.17
$CaCl_2$	8.5	75.6	15.1	0.0	0.0	0.0	0.3	0.5	0.20
$FeCl_2$	9.6	61.9	26.0	0.0	1.4	0.0	1.1	0.0	0.42
$BaCl_2$	9.3	75.9	13.7	0.0	0.0	0.7	0.4	0.0	0.18

[a]Unexposed PPS surface.

TABLE V Chemical composition of PTFE-blended PPS surfaces after exposure for 21 days to 1 M various chloride reactants at 200°C

Chloride reactant	Atomic fraction, %									Atomic ratio, O/C
	S	C	O	F	Na	Fe	Ba	Cl	Ca	
Control[a]	2.5	45.7	3.0	48.8	0.0	0.0	0.0	0.0	0.0	0.07
D.I. water	2.1	39.8	3.0	55.1	0.0	0.0	0.0	0.0	0.0	0.08
NaCl	2.3	39.6	3.4	54.7	0.0	0.0	0.0	0.0	0.0	0.09
$CaCl_2$	2.2	39.6	2.6	55.6	0.0	0.0	0.0	0.0	0.0	0.07
$FeCl_2$	2.1	39.5	3.9	54.4	0.0	0.0	0.0	0.0	0.0	0.10
$BaCl_2$	2.4	37.5	4.2	55.9	0.0	0.0	0.0	0.0	0.0	0.11

[a]Unexposed PTFE-blended PPS surface.

(Table IV) were exposed to hot deionized (D.I.) water as reference solution, their surfaces underwent some hydrothermal oxidation, reflecting the O/C atomic ratio of 0.14, which is two times higher than that of the unexposed control surfaces. By comparison, the incorporation of more oxygen into the film surfaces was detected from the samples exposed to the chloride solutioins, leading to the O/C ratio of >0.17. Considerable attention was paid to the film surfaces exposed to $FeCl_2$ solution because they had the highest O/C ratio of 0.42. This finding is taken as evidence that $FeCl_2$ enhances the degree of oxidation of the PPS surfaces. For comparing the value of O/C ratio, the ranking of the reactivity of PPS with these chloride reactants was in the following order: $FeCl_2 > CaCl_2 > BaCl_2 > NaCl$. The data also showed that the amount of Cl migrating from the $FeCl_2$ solution to the film surfaces was much higher than that for the other chlorides, suggesting that the oxidation of PPS by $FeCl_2$ may lead to the formation of polychloroaryl derivative.

In contrast, blending the PTFE significantly served in reducing the degree of oxidation of the PPS. As is seen in Table V, no significant difference in the O/C ratio was observed from all the PTFE-blended PPS coatings after exposure to these chloride reactants, compared with that of the unexposed ones. Also, Na, Fe, Ba, Cl, and Ca atoms were not detected on the exposed coating surfaces. It is apparent that the PTFE surface layer greatly inhibits the hydrothermal oxidation reaction of the film surfaces with hot chloride solution.

4. Conclusion

In formulating and designing scale-free polymeric material systems with heat-transferable properties for use as interior surface coatings of the heat exchanger tubes made from mild carbon steel (MCS), we evaluated the three coating systems; SiC-filled trimethylopropane trimethacrylate-crosslinked styrene/methyl methacrylate (TMP-ST) copolymer containing 1,4-phenylene diamine (PDA) antioxidant, SiC-filled polyphenylene sulfide (PPS), and unfilled polytetrafluoroethylene (PTFE)-blended PPS. These coatings were deposited onto zinc phosphate-treated MCS tubes and tested for assessing their abilities to protect the underlying MCS against corrosion, to minimize the degree of hydrothermal oxidation of coating surfaces, and to transfer heat. Tests were carried out in the geothermal power plants for 45 days at temperatures up to 110°C. Although all of the coatings had an adequate heat-transfer property and an excellent corrosion-preventing barrier, the degree of hydrothermal oxidation of the coating surfaces was a critical issue in preventing their chemical affinity for the geothermal brine-induced scale deposits. PDA antioxidant had no significant effect on inhibiting oxidation of the TMP-ST thermoset coating system, thereby resulting in a strong bond at the interfaces between scales and coating surfaces that make it difficult to remove the scales. In contrast, a very promising coating which ensures that the scale layers can be dislodged by highly pressurized water, was successfully fabricated using the PPS and PTFE-blended PPS thermoplastic polymers, reflecting a lower shear bond strength at the scale/coating joints. However, one major concern about the hydrothermal oxidation of PPS was the fact that its surfaces preferentially react with the $FeCl_2$ which is one of the chemical components of geothermal brine. This reaction promoted the degree of oxidation of PPS, resulting in the conformational transformation of sulfide within the PPS into sulfone. A further oxidation of polysulfone caused the disintegration of PPS structure into fragmental polysulfonic acid and aryl radical derivatives. Furthermore, incorporating more oxygen into the disintegrated PPS led to the decomposition of polysulfonic acid to generate H_2SO_4. Finally, the interactions between H_2SO_4, $FeCl_2$, and aryl radicals, led to the formation of $FeSO_4$ and polychoroaryl derivatives as reaction products. Since $FeSO_4$ is soluble in water, there was no problem in removing it from the coating surfaces by pressurized water.

On the other hand, blending PTFE into the PPS offered improved oxidation resistance of the coating surfaces. The main reason for such improvement was due to the phase segregation of PTFE from the PPS, whereby self-segregated PTFE formed the outermost surface layer of coating. The susceptibility of PTFE to the hydrothermal reactions with hot brine was considerably lower than that of the PPS, forming surfaces that were chemically inert to the scales. Thus, the scales easily flaked off from the coating surfaces.

References

1. J. J. FONTANA, W. REAM and H. C. CHENG, in "5th International Congress on Polymer in Concrete," edited by B. W. Staynes (Brighton Polytechnic, Brighton, 1987) p. 399.
2. V. HASSANI and E. HOO, National Renewable Energy Laboratory (NREL) Technical Report, Golden, Colorado, November, 1995.
3. T. SUGAMA, *Geothermics* **27** (1998) 387.
4. M. S. REISCH, *Chem. Eng. News* **71** (1993) 24.
5. D. W. DWIGHT and W. M. RIGGS, *J. Colloid and Interface Sci.* **47** (1974) 651.

6. C. R. SHASTRY and H. E. TOWNSEND, *Corrosion* **45** (1987) 100.
7. R. SARD, *Plating and Surface Finishing* **74** (1987) 30.
8. T. SUGAMA and N. R. CARCIELLO, *Int. J. Adhesion and Adhesives* **11** (1991) 97.
9. K. GAWLIK, T. SUGAMA, R. WEBSTER and W. REAMS, in Geothermal Annual Meeting, September 20–23 1999, SanDiego, CA. *Geothermal Resources Council Transaction*, **22**, in press.
10. C. D. WAGNER, W. M. RIGGS, L. E. DAVIS, J. F. MOULDER and G. E. MUILENBERG, "Handbook of X-ray Photoelectron Spectroscopy" (Perkin-Elmer Corporation, Eden Prairie, Minnesota, 1979) p. 17.
11. J. RIGA, J. P. BOUTIQUE and J. J. VERBIST, "Physic-ochemical Aspects of Polymer Surfaces," edited by K. L. Mittal (Plenum Press, New York, 1983) p. 45.
12. B. J. LINDBERG, K. HAMRIN, G. JOHNASSON, U. GELIUS, A. FAHLMAN, C. NORDLING and K. SIEGBAHN, *Physical Scripta.* **1** (1970) 286.
13. C. E. MIXAN and J. B. LAWBERT, *J. Org. Chem.* **38** (1975) 1350.
14. Y. LIMOUNZIN-MAIRE, J. C. MAIRE and A. BALDY, *Bull. Cercle Etud. Met.* **14** (1981) 1.
15. R. W. LENZ and J. CARRINGTON, *J. Poly. Sci.* **41** (1959) 333.
16. *Idem., ibid.* **43** (1960) 167.
17. D. T. CLARK, D. KILCAST and W. K. R. MUSGRAVE, *J. Chem. Soc.* **10** (1971) 516.

Received 28 June
and accepted 21 October 1999